NEIGHBORING PANELS BLOCKING AND DIFFRACTION EFFECTS ON THE PERFORMANCE OF THE SMALL FLAT MULTI-PANEL RECONFIGURABLE REFLECTOR ANTENNA

Suphachet PHERMPHOONWATANASUK, and Chatchai WAIYAPATTANAKORN
Electrical Engineering Department Chulalongkorn University Phyathai Road Patumwan Bangkok Thailand 10330
Tel. (662) 2186502 Fax. (662) 2518991 E-mail: g3966433@student3.netserv.chula.ac.th

Abstract

Beam reconfiguration by structural reconfigurable antenna, such as the small flat multi-panel reconfigurable reflector antenna, has an aspect of great concern that is the effects due to the use of a number of small panels to form the reflecting surface. This paper has emphasis on theoretical study of neighboring panels blocking and diffraction effects on the small flat multi-panel reconfigurable reflector antenna's performance. The "null-field hypothesis" and the physical theory of diffraction (PTD) are used to account for the effect of both phenomena on the ability in steering the main beam and the contribution to the cross-polar component. It is found that the main contribution to the total cross polarization is depolarization due to the finite size of the panels. The maximum cross-polar gain predicted using PTD is around –30 dB. The neighboring panels blocking causes distortion on the co-polar pattern for the observer far off the boresight.

I. Introduction

The structural reconfigurable reflector antenna can be used to produce the beam shape in response to changing transmission demands [1,2] and can create nulls in order to counter the interference between different signal frequencies [3,4]. In addition, it can steer the main beam to the desired direction [5,6]. An advantage of this antenna is, it does not need any complex feed network that introduces high loss or phase shift of the transmitted or the received signals. However it has some disadvantage due to interpanel gap loss, edge diffraction, and blocking from the surrounding panels. In this paper the effect of edge diffraction and blocking on the ability in steering the main beam and the contribution to the cross-polar levels are investigated. The methods for accounting the neighboring panels blocking and the depolarizing effects of their edges are the "null-field hypothesis" [7] and the physical theory of diffraction (PTD) [8,9]. The null field hypothesis assumes that no currents are excited on the shadowed panel cast by the neighboring panels, and the currents do not radiate in the observation point direction. The ray approximation technique [6] is used to steer the main beam by approximating the direction of the ray bundles that can possibly form the desired beam direction.

II. The Small Flat Multi-Panel Reconfigurable Reflector Antenna

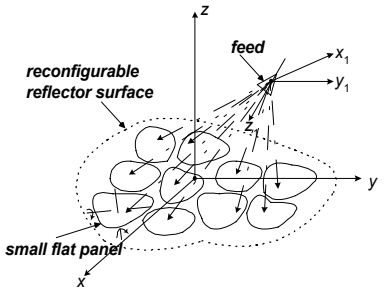

Fig 1. Structure of a small flat multi-panel reconfigurable reflector antenna.

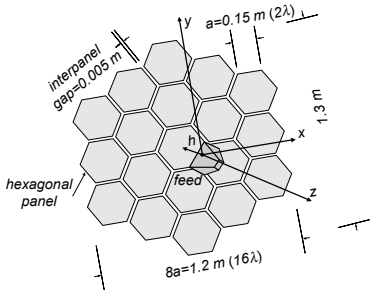

Fig. 2. The reconfigurable reflector surface.

Beam reconfiguration of the small flat multi-panel reconfigurable reflector antenna is achieved by changing the reflector surface. As shown in Fig. 1, this antenna is a sub-category of the reflector antenna which the flexible reflector is approximated by many small flat panels. The approximate surface can reradiate the incident energy of the feed and form the desired beam shape and direction by adjusting all panels mechanically.

In this work the reconfigurable reflector nominal surface is flat circular, with its surface divided into a number of hexagonal panels as shown in Fig. 2. A single linearly polarized feed is placed at a position that ensures symmetrical illumination on the reflector surface. The operating frequency is set to 4 GHz. The rotation angle of each panel is set to be less than 45 degrees.

The following feed radiation pattern has been assumed in the analysis:

$$\vec{E}^{feed}(r_1,\theta_1,\phi_1) = \left[f_E(\theta_1)\sin\phi_1\hat{\theta}_1 + f_H(\theta_1)\cos\phi_1\hat{\phi}_1\right]\frac{e^{-jkr_1}}{r_1},\quad \vec{H}^{feed}(r_1,\theta_1,\phi_1) = \left[\frac{f_E(\theta_1)\sin\phi_1\hat{\phi}_1 - f_H(\theta_1)\cos\phi_1\hat{\theta}_1}{Z_o}\right]\frac{e^{-jkr_1}}{r_1} \quad (1)$$

where $f_E(\theta_1) = \cos^{q_e}\theta_1$, $f_H(\theta_1) = \cos^{q_h}\theta_1$, Z_o is the free space wave impedance, and k is the wave number.

III. Analysis Method

The analytical procedure is shown in Fig. 3. The physical optics expression for the electric fields radiated from the reconfigurable reflector surface is given by

$$\vec{E}^{PO}(\vec{r}) \overset{R\to\infty}{\cong} -\frac{j\omega\mu e^{-jkr}}{4\pi r}\sum_{m=1}^{M_s}\iint_{S_m}\left[\vec{J}_m^{PO}-(\vec{J}_m^{PO}\cdot\hat{r})\hat{r}\right]e^{jk(\vec{r}_m^{\,s}\cdot\hat{r})}dS_m \tag{2}$$

where $\vec{J}_m^{PO}(\vec{r}_m^{\,s})=2\hat{n}_m\times\vec{H}^{feed}(\vec{r}_m^{\,s})$ is the physical optics currents, $\vec{r}_m^{\,s}$ describes the points on the panel surface S_m, $\vec{r}$ describes the observation points, $\vec{R}=\vec{r}-\vec{r}_m^{\,s}$, and $R=|\vec{R}|$.

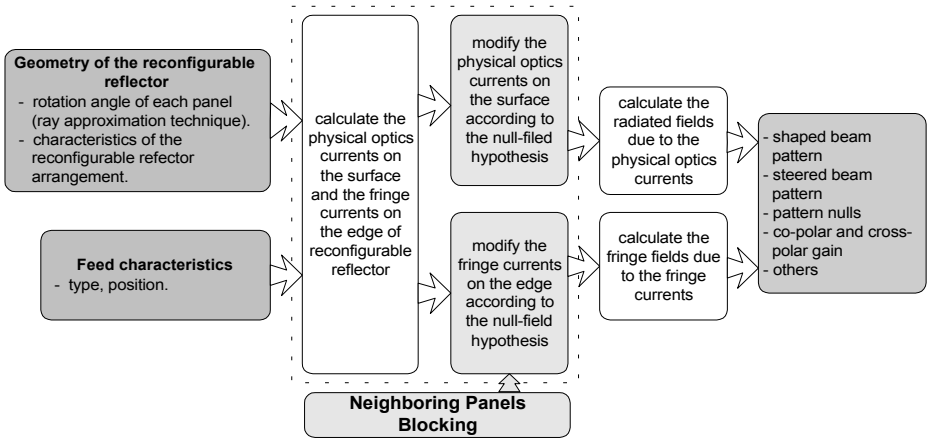

Fig. 3. Analytical procedure.

The fringe fields radiated from the edges of each panel can be obtained by employing the PTD, thus

$$\vec{E}^{fr}(\vec{r})\cong jk\sum_{m=1}^{M_e}\oint_{C_m}\left[Z_o I_m^{fr}\hat{s}_m\times(\hat{s}_m\times\hat{e}_m)+M_m^{fr}\hat{s}_m\times\hat{e}_m\right]\frac{e^{-jkr}}{4\pi r}dl_m \tag{3}$$

where $I_m^{fr}=I_m^{T}-I_m^{PO}$, $M_m^{fr}=M_m^{T}-M_m^{PO}$,

$$I_m^{T}=\frac{2j\vec{H}^{feed}\cdot\hat{e}_m}{k\sin\beta'}\frac{\mu\cot\beta'-\cot\beta\cos\phi}{\cos\phi'+\mu}\frac{\sqrt{2}\cos\left(\frac{\phi'}{2}\right)}{\sqrt{1-\mu}}+\frac{2jY_o\vec{E}^{feed}\cdot\hat{e}_m}{k\sin^2\beta'}\frac{\sqrt{2}\sin\left(\frac{\phi'}{2}\right)}{\cos\phi'+\mu}\sqrt{1-\mu},$$

$$I_m^{PO}=\left[-\frac{2j\vec{H}^{feed}\cdot\hat{e}_m}{k\sin\beta'}\frac{\cot\beta'\cos\phi'+\cot\beta\cos\phi}{\cos\phi'+\mu}+\frac{2jY_o\vec{E}^{feed}\cdot\hat{e}_m}{k\sin^2\beta'}\frac{\sin\phi'}{\cos\phi'+\mu}\right]\left[U(\pi-\phi')-U(\phi'-\pi)\right],$$

$$M_m^{T}=-\frac{2jZ_o\vec{H}^{feed}\cdot\hat{e}_m}{k\sin\beta'\sin\beta}\frac{\sin\phi}{\cos\phi'+\mu}\frac{\sqrt{2}\cos\left(\frac{\phi'}{2}\right)}{\sqrt{1-\mu}},\ M_m^{PO}=-\frac{2jZ_o\vec{H}^{feed}\cdot\hat{e}_m}{k\sin\beta'\sin\beta}\frac{\sin\phi}{\cos\phi'+\mu}\left[U(\pi-\phi')-U(\phi'-\pi)\right],$$

$$\mu=\frac{\sin\beta\cos\phi+\cot\beta'(\cos\beta-\cos\beta')}{\sin\beta'},\ \alpha=\cos^{-1}\mu=-j\ln(\mu+\sqrt{\mu^2-1}),\ \beta=\pi-\cos^{-1}(\hat{s}_m\cdot\hat{e}_m),$$

$$\beta'=\pi-\cos^{-1}(\hat{s}'_m\cdot\hat{e}_m),\ \hat{\phi}_m=\frac{\hat{s}_m\times\hat{e}_m}{\|\hat{s}_m\times\hat{e}_m\|},\hat{\beta}=\hat{s}_m\times\hat{\phi}_m,\ \hat{\phi}'_m=\frac{\hat{e}_m\times\hat{s}'_m}{\|\hat{e}_m\times\hat{s}'_m\|},\hat{\beta}'=\hat{s}'_m\times\hat{\phi}'_m,$$

$$\phi=\begin{cases}\cos^{-1}(\hat{n}_m\cdot\hat{\phi}_m), & \hat{t}_m\cdot\hat{\phi}_m\le 0\\ 2\pi-\cos^{-1}(\hat{n}_m\cdot\hat{\phi}_m), & \hat{t}_m\cdot\hat{\phi}_m>0\end{cases},\ \phi'=\begin{cases}\cos^{-1}(\hat{n}_m\cdot\hat{\phi}'_m), & \hat{t}_m\cdot\hat{\phi}'_m\le 0\\ 2\pi-\cos^{-1}(\hat{n}_m\cdot\hat{\phi}'_m), & \hat{t}_m\cdot\hat{\phi}'_m>0\end{cases},$$

$\hat{s}'_m$ is the unit vector from the feed to the m^{th} edge, $\hat{s}_m$ is the unit vector from the m^{th} edge to the observer, $\hat{e}_m=-\vec{r}'/\|\vec{r}'\|$ is the unit vector tangent to the m^{th} edge, $\hat{n}_m$ is the unit normal vector of the panel, $\hat{t}_m=\hat{e}_m\times\hat{n}_m$ is the unit tangent vector of the panel outward from the m^{th} edge to the surface, and $U(\bullet)$ is the unit step function.

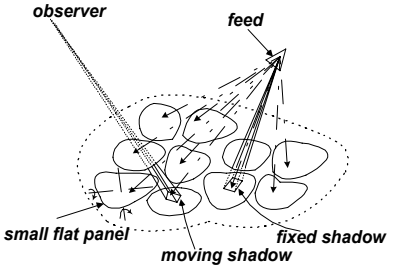

Fig. 4. Neighboring panels blocking.

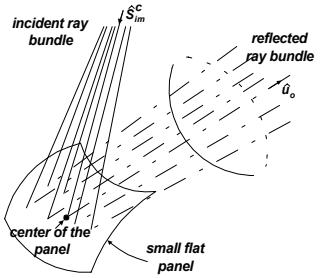

Fig. 5. Ray approximation technique.

For neighboring panels blocking, after each panel has been adjusted, two types of shadows are cast on the panel according to the null-field hypothesis as shown in Fig 4.

1) Fields radiated from the feed may be blocked by neighboring panels. It causes no currents excited on some regions of the panel. This region is called the "fixed shadow" because the shadows do not migrate except when the feed is scanned.
2) Fields radiated from the panel may be obstructed by the surrounding panels. It causes no radiation in the observation direction as if there was no currents when observe from that observation point. This region is called the "moving shadow" because the shadows move when the observer location changes.

From this hypothesis, the estimation of the blocking effects can be obtained by setting the physical optics currents and the fringe currents on the panel to zero if these currents flow on the fixed and the moving shadow.

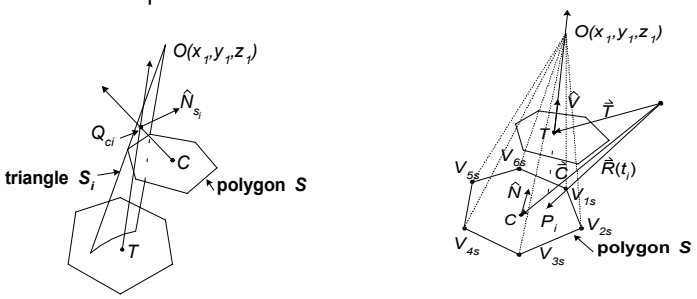

Fig. 6. Checking for shadow casting.

Fig. 6 shows how one can check for shadow casting by surrounding panels. *T* is the test point on the panel. S_i is the triangle formed by the i^{th} side of the polygon *S* and a distant observation point or the feed position $O(x_1,y_1,z_1)$. *C* is the center point of the polygon *S*. Q_{ci} is the center point of the triangle S_i. *T* is on the same side with *C* on all sides of the polygon *S* if

$$\Omega_{Ti}\Omega_{Ci} \geq 0, \qquad 1 \leq i \leq N_s \tag{4}$$

where $\Omega_{Ti} = \frac{(\vec{Q}_{ci} - \vec{T})}{||\vec{Q}_{ci} - \vec{T}||} \cdot \hat{N}_{s_i}$, $\Omega_{Ci} = \frac{(\vec{Q}_{ci} - \vec{C})}{||\vec{Q}_{ci} - \vec{C}||} \cdot \hat{N}_{s_i}$, N_s is the number of sides of the polygon *S*, $\hat{N}_{s_i}$ is the unit normal vector of the triangle S_i and will lie in the shadow of the polygon *S* when the intersection point P_i of the ray $\vec{R}(t_i) = \vec{T} + t_i\hat{V}$ on the polygon *S* is in front of *T* and along the ray $\hat{V}$. This situation can be expressed as follows:

$$t_i = \frac{(\vec{V}_{1s} - \vec{T}) \cdot \hat{N}}{\hat{N} \cdot \hat{V}} \tag{5}$$

where $\hat{N} = \frac{(\vec{V}_{2s} - \vec{V}_{3s}) \times (\vec{V}_{1s} - \vec{V}_{2s})}{||(\vec{V}_{2s} - \vec{V}_{3s}) \times (\vec{V}_{1s} - \vec{V}_{2s})||}$ is the unit vector normal to the polygon *S*, V_{1s}, V_{2s}, V_{3s} are the vertices of the polygon *S*, and $\hat{V} = \frac{\vec{O} - \vec{T}}{||\vec{O} - \vec{T}||}$ is the unit vector from *T* to *O*.

If $\hat{N} \cdot \hat{V} = 0$ then the ray $\hat{V}$ is parallel to the polygon *S* where $(\vec{C} - \vec{T}) \cdot \hat{V} > 0$, *T* lies in the shadow and $(\vec{C} - \vec{T}) \cdot \hat{V} < 0$, *T* is outside the shadow else if $t_i \leq 0$ then the intersection point is behind *T* (*T* outside the shadow) else the intersection point is in front of *T* (*T* lies in the shadow).

In order to steer the beam to the desired direction, the ray approximation technique is used to find the rotation angle of the panels. It is assumed that the reflected ray bundles have the same wave front as the reflected ray at the center of the panel as shown in Fig. 5. The rotation angle of each panel can be obtained by

$$\hat{n}_m = \frac{\hat{u}_o - \hat{s}^c_{im}}{||\hat{u}_o - \hat{s}^c_{im}||}, \ \theta^{rot}_m = \tan^{-1}\left(\frac{\sqrt{n^2_{mx} + n^2_{my}}}{n^2_{mz}}\right), \ \phi^{rot}_m = \tan^{-1}\left(\frac{n_{my}}{n_{mx}}\right) \tag{6}$$

where $\hat{u}_o = \sin\theta_o\cos\phi_o\hat{x} + \sin\theta_o\sin\phi_o\hat{y} + \cos\theta_o\hat{z}$ is the unit vector in the desired direction (θ_o, ϕ_o), $\hat{s}^c_{im}$ is the unit vector of the incident ray at the center of the m^{th} panel, and $\theta^{rot}_m, \phi^{rot}_m$ are the rotation angle about the elevation and the azimuthal axes of the m^{th} panel respectively.

For the flat shape case, the accuracy of the ray approximation technique for steering the beam depends upon the feed position (*h*). Numerical investigations [5,6] show that the suitable feed position is about 1.1-1.2 times of the radius of the reconfigurable reflector.

IV. Numerical Results

The purpose of the numerical calculations is to illustrate the effects of both the edge diffraction and the neighboring panels blocking on the co-polar and cross-polar patterns. The reconfigurable reflector studied consists of 19 hexagonal panels and the dimension of the reconfigurable reflector is shown in Fig. 2. The illuminating field is a y-polarized raised cosine order 2 feed. Fig. 7-10 show the effects of both phenomena on the ability in steering the main

beam to 0, 20, 40, and 60 degrees from boresight. It is found that the main contribution to the total cross polarization is depolarization due to the finite size of the panels. The PTD predictions of the cross-polar gain are larger than those obtained using PO. The PO predictions of the cross-polar gain are very low (not shown in the figure). Relative to the maximum co-polar gain the maximum cross-polar gain predicted using PTD is around –30 dB. The blocking effects have minor influence on the cross-polar pattern. Both phenomena cause distortion on the co-polar pattern for the observer far from booresight but the neighboring panel blocking has more influence than the edge diffraction. The high sidelobe levels are due to the flat reconfigurable reflector surface. From Fig. 9-10 it is seen that the spikes occur in the pattern may be due to the Ufimtsev singularity of the untruncated EEC's.

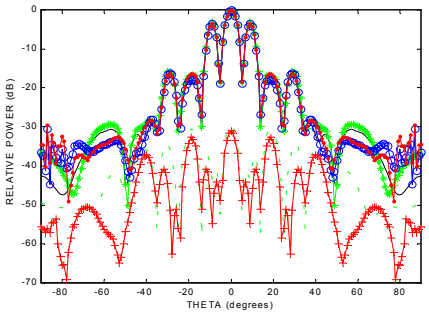

Fig. 7. 0 degrees steering pattern.

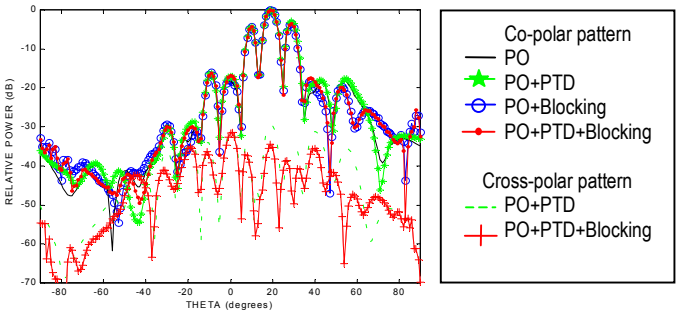

Fig. 8. 20 degrees steering pattern.

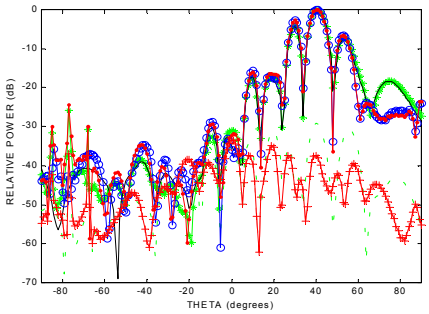

Fig. 9. 40 degrees steering pattern.

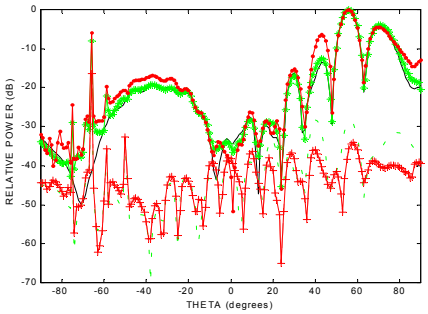

Fig. 10. 60 degrees steering pattern.

V. Conclusion

In this paper, neighboring panels blocking and diffraction effects on beam steering of the reconfigurable reflector antenna has been studied. From numerical results, the blocking effects have minor influence on cross-polarization. The panel's edge diffraction is the main contribution to the total cross polarization. Both effects cause distortion on the co-polar pattern for the observer far from boresight but the neighboring panels blocking has more influence than the edge diffraction. In the future, the antenna pattern will be measured to compare with these results.

Acknowledgement

The authors acknowledge the partial support of this project by the Sit-Kon-Kuti programme Chulalongkorn University and the National Science and Technology Development Agency, and the ASAHI glass foundation.

References

[1] P.J.B. Clarricoats, and H. Zhou, 'Design and performance of a reconfigurable mesh reflector antenna. Part 1: Antenna Design,' *IEE Proc. Part H.*, vol. 138, (6), pp. 485-492, 1991.

[2] R.C. Brown, 'A reconfigurable reflector using hinged panels,' *Proc of IEE International Conf. Antennas Propagat.*, pp. 531-534, 1991.

[3] A.D. Monk, and P.J.B. Clarricoats, 'Reconfigurable reflector antenna producing pattern nulls,' *IEE Proc. Part H.*, vol. 142, (2), pp. 121-128, 1995.

[4] M. Indravuth, C. Waiyapattanakorn, and S. Phermphoonwatanasuk, 'Smart antenna versus structural reconfigurable antenna,' *International Wireless and Telecommunications Symposium/Exhibition (IWTS).*, vol. 1, pp. 128-130, 1999.

[5] S. Phermphoonwatanasuk, and C. Waiyapattanakorn, 'Small flat multi-panel reconfigurable reflector antenna: theoretical investigation,' *Progress In Electromagnetics Research Symposium (PIERS).*, pp. 346, 1998.

[6] S. Phermphoonwatanasuk, and C. Waiyapattanakorn, 'The flat reconfigurable paneled reflector antenna,' *20th Electrical Engineering Conference.*, Thailand, pp. 686-691, 1997.

[7] W.V.T. Rusch, L.R. Welch, and G.E. Mires, 'Observation-point-dependent blocking shadows on a reflector antenna,' *IEEE Trans. Antennas Propagat.*, Vol. AP-37, pp. 690-697, 1989.

[8] A. Michaeli, 'Equivalent edge currents for arbitrary aspects of observation,' *IEEE Trans. Antennas Propagat.*, Vol. AP-32, pp. 252-258, 1984.

[9] A. Michaeli, 'Elimination of infinities in equivalent edge currents, Part I: fringe current components,' *IEEE Trans. Antennas Propagat.*, Vol. AP-34, pp. 912-918, 1986.